Bioactivity of Fe_2O_3-containing $CaO–SiO_2$ glasses: *in vitro* evaluation

Y. EBISAWA*, T. KOKUBO
Institute for Chemical Research, Kyoto University, Uji, Kyoto-Fu 611, Japan
K. OHURA, T. YAMAMURO
Department of Orthopaedic Surgery, Faculty of Medicine, Kyoto University, Sakyo-Ku, Kyoto-City 606, Japan

In order to reveal conditions for obtaining bioactive and ferrimagnetic glass-ceramics useful as thermoseeds for hyperthermia treatment of cancer, the effects of additives on the bioactivity of an $Fe_2O_3–CaO–SiO_2$ glass were investigated by examining apatite formation on the surfaces of the glasses in a simulated body fluid with ion concentrations nearly equal to those in human blood plasma. A $3Fe_2O_3$, $100CaO \cdot SiO_2$ (in weight ratio) glass did not form an apatite layer on its surface in the fluid, but glasses of the same compositions with $3Na_2O$, B_2O_3 and/or P_2O_5 added (in weight ratio) formed an apatite layer. This indicates that bioactive and ferrimagnetic glass-ceramics could be obtained from Fe_2O_3-containing $CaO–SiO_2$ glasses with Na_2O, B_2O_3 and/or P_2O_5 added. Apatite formation on the surfaces of the glasses with the additives are interpreted in terms of the dissolution of the calcium and silicate ions from the glasses.

1. Introduction

It was previously shown by our group that even P_2O_5-free $CaO–SiO_2$ glasses bond to living bone, forming an apatite layer on their surfaces in the body [1–3]. This indicates a possibility that a bioactive and ferrimagnetic glass-ceramic which contains ferrimagnetic magnetite (Fe_3O_4) in a bioactive CaO,SiO_2-based crystalline or glassy matrix could be obtained by crystallization of $CaO–SiO_2$ glasses containing appreciable amounts of FeO and Fe_2O_3. Such glass-ceramic might be useful as thermoseeds for hyperthermia treatment of cancer, especially bone tumour, since it bonds to itself as well as to living bone to be fixed, and heats the surrounding bone locally to temperatures effective for cancer treatment by magnetic hysteresis loss under an alternating magnetic field. Heat treatment of a glass of nominal composition (wt %) Fe_2O_3 40, $CaO \cdot SiO_2$ 60 at 950 °C gave a glass-ceramic which contained about 36 wt % magnetite in a matrix of β-wollastonite ($CaO \cdot SiO_2$) and a CaO,SiO_2-based glassy phase [4]. Thus, the glass-ceramic obtained showed ferrimagnetism, as expected. It did not, however, show bioactivity, since the glassy phase contained a small amount of Fe_2O_3 [4]. It is already known that the bioactivity of the $CaO–SiO_2$ glass is lost by the addition of a small amount of Fe_2O_3 [1, 3].

In this study, in order to reveal the conditions for obtaining bioactive and ferrimagnetic glass-ceramic, the effects of various additives on apatite formation on the surface of an $Fe_2O_3–CaO–SiO_2$ glass in a simulated body fluid were investigated.

It has already been shown for various kinds of glasses and glass-ceramics that materials forming an apatite layer on their surfaces in simulated body fluid with ion concentrations nearly equal to those of human blood plasma bond to the bone through the same kind of apatite layer formed in the living body [1–3, 5–13].

2. Experimental

2.1. Preparation of glasses

The nominal compositions of the glasses examined are shown in Table I. About 30 g powder mixtures of these compositions were prepared from reagent grade $CaCO_3$, SiO_2, Fe_2O_3, Na_2CO_3, H_3BO_3 and $CaHPO_4 \cdot 2H_2O$. They were placed in a platinum crucible and melted in an $MoSi_2$ electric furnace at 1550 °C for 2 h. The melts were poured on to a stainless steel plate at room temperature and pressed into a plate 1–2 mm thick. The glasses obtained were cut into a rectangular specimen 10 mm × 15 mm × 1 mm and polished with 1 μm diameter diamond paste.

2.2. Soaking in a simulated body fluid

The glass specimens were cleaned with acetone in an ultrasonic cleaner and immersed in 35 ml simulated body fluid which had ion concentrations almost equal to those of human blood plasma [14], as shown in Table II. The fluid was prepared by dissolving reagent grade NaCl, $NaHCO_3$, KCl, $K_2HPO_4 \cdot 3H_2O$,

*On leave from: Sumitomo Metal Industries, Ltd, Otemachi, Tokyo 100, Japan.

0957–4530

$MgCl_2 \cdot 6H_2O$, $CaCl_2$ and Na_2SO_4 in distilled water. It was buffered at pH 7.25 with 50 mM tris-(hydroxymethyl)-aminomethane $[NH_2C(CH_2OH)_3]$ and 45 mM hydrochloric acid (HCl). The temperature of the fluid was maintained at 36.5 °C. No living cell or organic substance was added.

2.3. Analysis of surface structure

At various daily intervals after the immersion, specimens were gently washed with acetone and their surfaces were analysed with thin-film X-ray diffraction and Fourier-transform infrared reflection spectroscopy. An X-ray diffractometer with a thin-film attachment (Rigaku model 2651A1) was used for the X-ray diffraction, in which the specimen surface was fixed at an angle of 1° to the incident beam. A Fourier-transform infrared spectrometer (Japan Spectroscopic FT-IR5M) was used for the infrared spectroscopy. The reflection angle was 75°. Both techniques enable analysis of a thin layer about 1 μm thick at the surface.

The specimens were embedded in polyester resin. Their cross-sections were polished with 1 μm diameter diamond paste, coated with a carbon film and then analysed with an electron-probe X-ray microanalyser (EPMA; Shimazu EPM-810). The electron beam was 0.3 μm in diameter and the accelerating voltage was 12.5 kV.

TABLE I Nominal compositions of the glasses examined

Glass	Composition (in weight ratio)				
	$CaO \cdot SiO_2$	Fe_2O_3	Na_2O	B_2O_3	P_2O_5
CS + Fe	100	3.0	0.0	0.0	0.0
CS + FeNa	100	3.0	3.0	0.0	0.0
CS + FeB	100	3.0	0.0	3.0	0.0
CS + FeP	100	3.0	0.0	0.0	3.0
CS + FeNaB	100	3.0	3.0	3.0	0.0
CS + FeNaP	100	3.0	3.0	0.0	3.0
CS + FeBP	100	3.0	0.0	3.0	3.0

3. Results and discussion

Figs 1–7 show the thin-film X-ray diffraction patterns and Fourier-transform infrared reflection spectra of the surfaces of the glasses soaked in the simulated body fluid for various periods. Assignments of the X-ray diffraction peaks and infrared reflection peaks were made according to the procedure described in the previous paper [7]. It can be seen from these figures that $3Fe_2O_3, 100CaO \cdot SiO_2$ (in weight ratio) glass with no additive does not form an apatite layer on its surface in the simulated body fluid even after 20 days, whereas the glasses of the same compositions with

TABLE II Ion concentrations of simulated body fluid and human blood plasma

	Concentration (mM)							
	Na^+	K^+	Ca^{2+}	Mg^{2+}	Cl^-	HCO_3^-	HPO_4^{2-}	SO_4^{2-}
Simulated body fluid	142.0	5.0	2.5	1.5	147.8	4.2	1.0	0.5
Human blood plasma	142.0	5.0	2.5	1.5	103.0	27.0	1.0	0.5

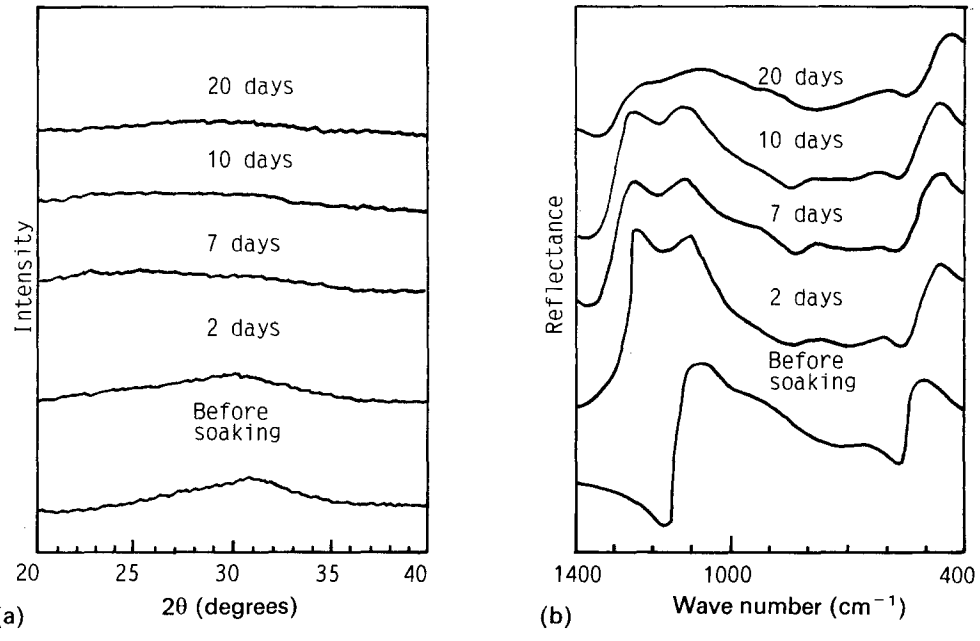

Figure 1 (a) Thin-film X-ray diffraction patterns and (b) Fourier-transform infrared reflection spectra of glass CS + Fe soaked in simulated body fluid for various periods.

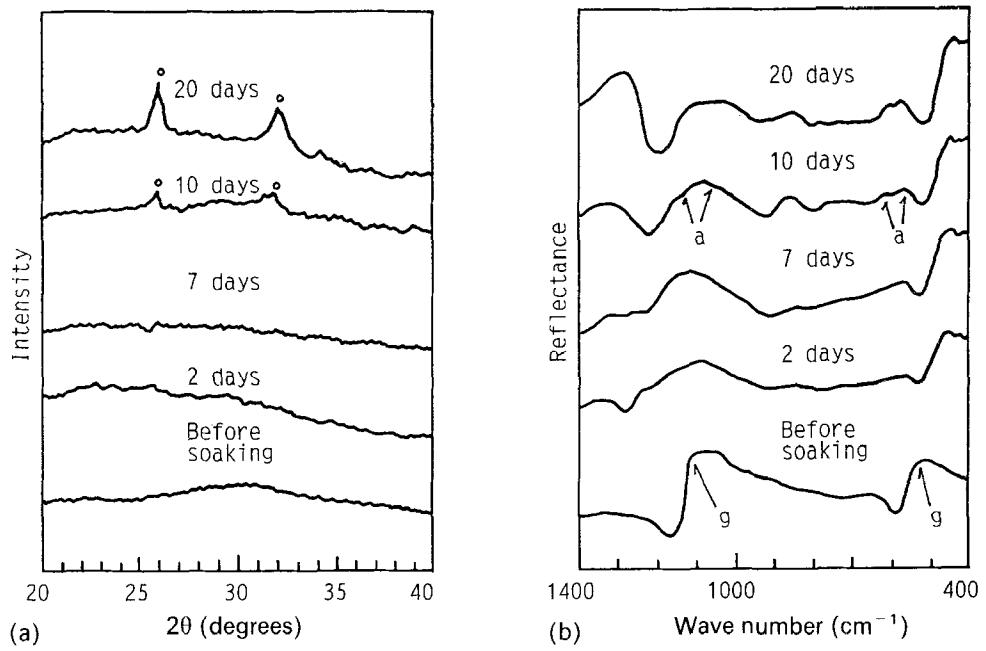

Figure 2 (a) Thin-film X-ray diffraction patterns and (b) Fourier-transform infrared reflection spectra of glass CS + FeNa soaked in simulated body fluid for various periods: ○, a, apatite and g, glassy phase.

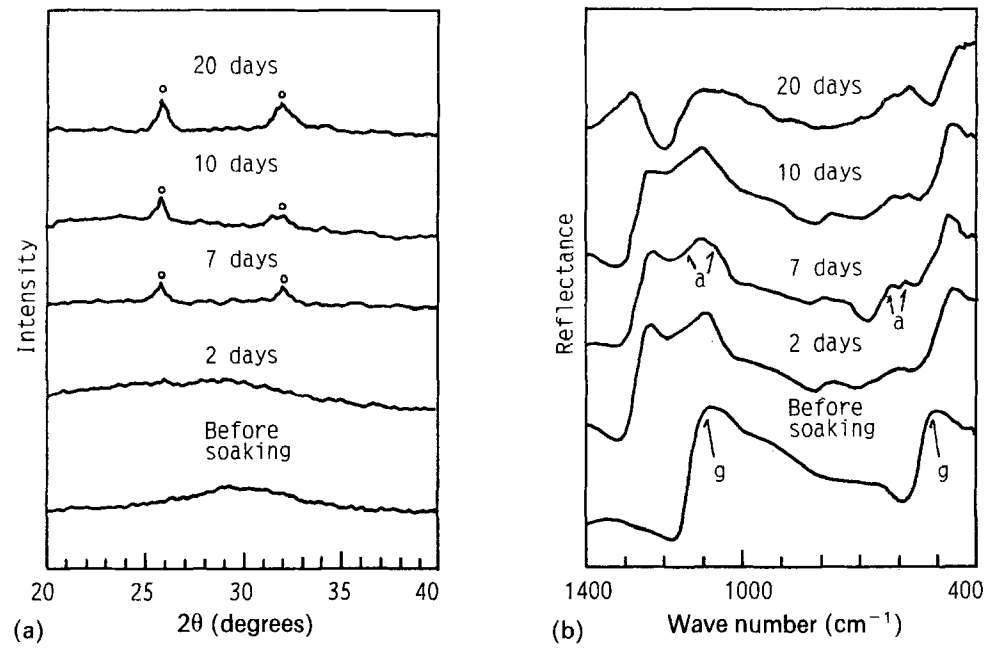

Figure 3 (a) Thin-film X-ray diffraction patterns and (b) Fourier-transform infrared reflection spectra of glass CS + FeB soaked in simulated body fluid for various periods: ○, a, apatite and g, glassy phase.

$3Na_2O$, B_2O_3 and/or P_2O_5 added (in weight ratio) all form a surface apatite layer. The rate of apatite formation increased in the order CS + FeP < CS + FeNa < CS + FeB < CS + FeNaB < CS + FeNaP < CS + FeBP. The lack of the apatite peaks on the X-ray diffraction patterns and infrared reflection spectra for CS + FeNaB and CS + FeNaP glasses soaked in the fluid for a long period is attributed to peeling off of the apatite layer before the surface analyses.

Figs 8–14 show the scanning electron microscopy (SEM) micrographs of cross-sections of the glasses soaked in the simulated body fluid for 20 days as well as the compositional profiles determined by the EPMA on the cross-section. The compositional profile of boron is not given in the figures, since the boron could not be detected by the apparatus used.

It can be seen from Figs 8–14 that $3Fe_2O_3$,$100CaO \cdot SiO_2$ (in weight ratio) glass with no additive shows hardly any compositional change on its surface even after being soaked in the simulated body fluid for 20 days, whereas the glasses of the same compositions with $3Na_2O$, B_2O_3 and/or P_2O_5 added (in weight ratio) all form an outermost layer rich in Ca and P and an underlying layer rich in Si on their surfaces. The Ca- and P-rich layer is ascribed to the apatite layer detected by the thin-film X-ray dif-

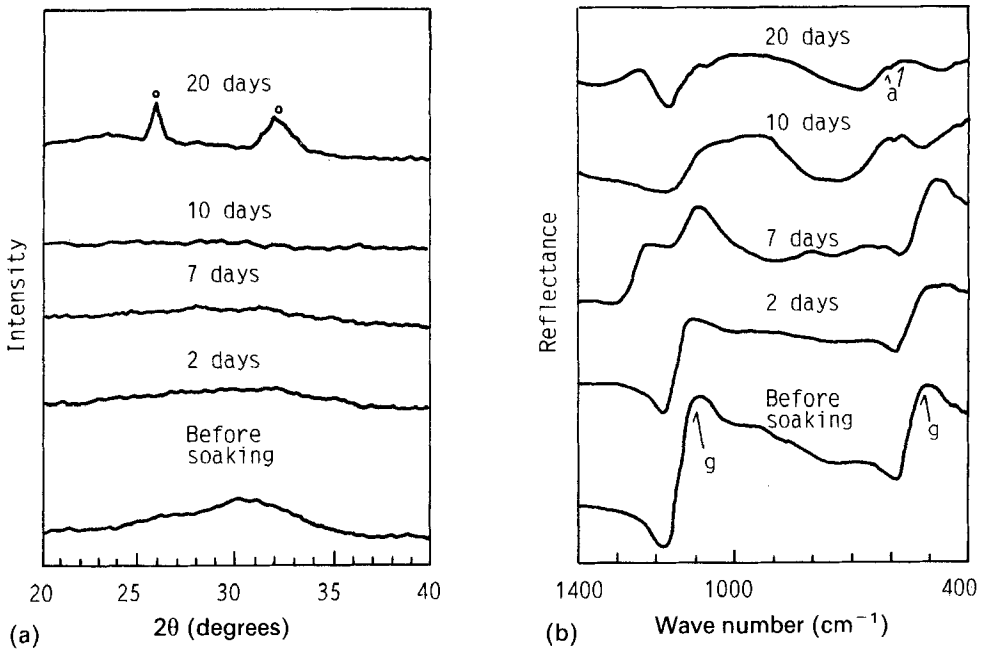

Figure 4 (a) Thin-film X-ray diffraction patterns and (b) Fourier-transform infrared reflection spectra of glass CS + FeP soaked in simulated body fluid for various periods: ○, a, apatite and g, glassy phase.

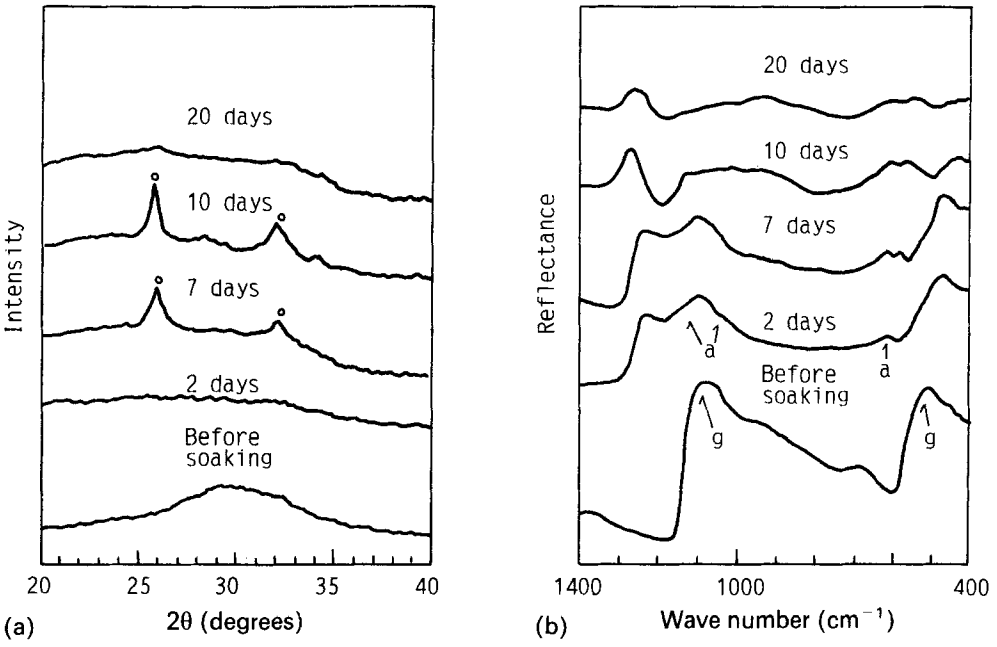

Figure 5 (a) Thin-film X-ray diffraction patterns and (b) Fourier-transform infrared reflection spectra of glass CS + FeNaB soaked in simulated body fluid for various periods: ○, a, apatite and g, glassy phase.

TABLE III Thickness of apatite and silica gel layers

Glass	Thickness (μm)	
	Apatite	Silica
CS + Fe	0	0
CS + FeNa	5	5
CS + FeB	5	7
CS + FeP	10	3
CS + FeNaB	7.5	7.5
CS + FeNaP	15	10
CS + FeBP	60	20

fraction and the infrared reflection spectroscopy. The Si-rich layer is ascribed to the same kind of silica hydrogel layer as that reported for Bioglass-type glasses [5, 15]. The thicknesses of the apatite and silica gel layers depended strongly on the composition of the glasses, as shown in Table III. It can be seen from Table III that the rate of formation of the apatite layer described above is proportional to the thickness of the silica gel layer. This might be interpreted as follows.

The silica gel layer is formed by selective dissolution of calcium ion from the glasses. The thickness of the silica gel layer increases with increasing rate of

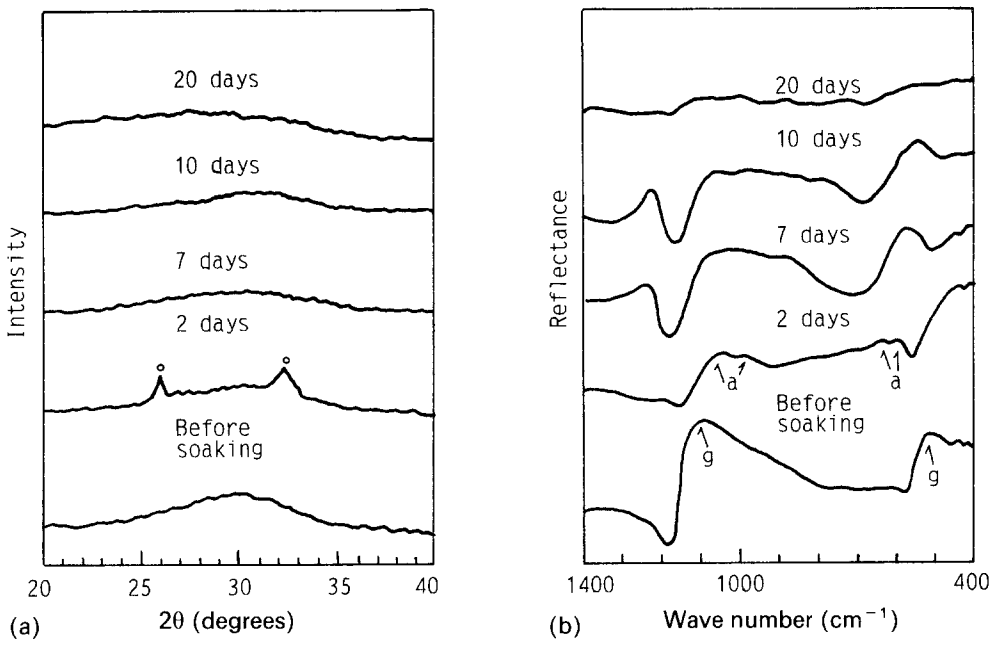

Figure 6 (a) Thin-film X-ray diffraction patterns and (b) Fourier-transform infrared reflection spectra of glass CS + FeNaP soaked in simulated body fluid for various periods: ○, a, apatite and g, glassy phase.

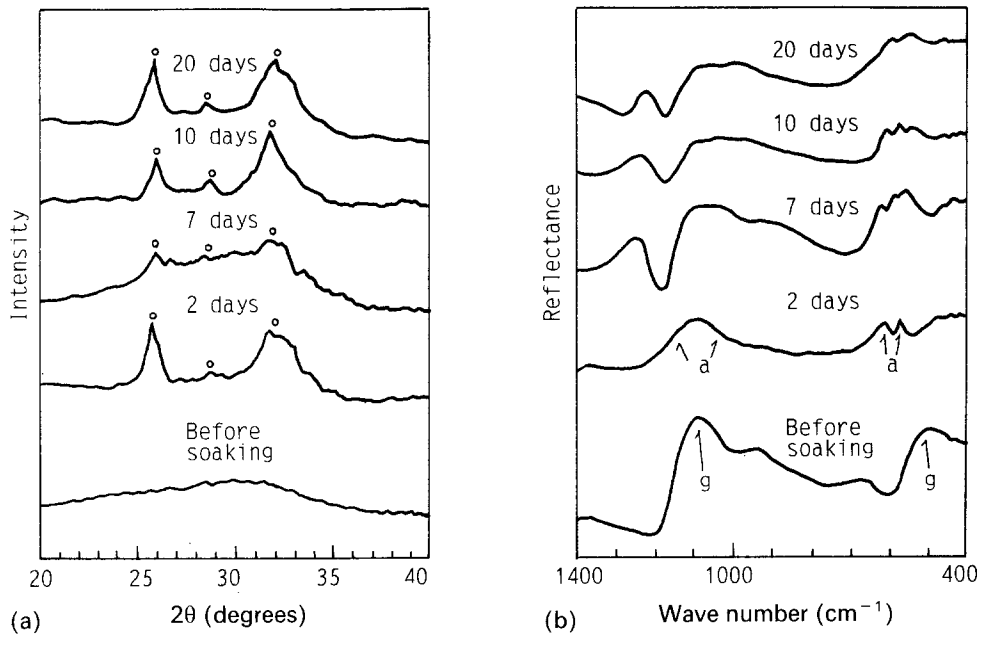

Figure 7 (a) Thin-film X-ray diffraction patterns and (b) Fourier-transform infrared reflection spectra of glass CS + FeBP soaked in simulated body fluid for various periods: ○, a, apatite and g, glassy phase.

dissolution of the calcium. Table III shows, therefore, that the rate of dissolution of the calcium increases in the order CS + Fe < CS + FeP < CS + FeNa < CS + FeB < CS + FeNaB < CS + FeNaP < CS + FeBP. The dissolved calcium ion increases the degree of the supersaturation of the surrounding fluid, which is already supersaturated with respect to the apatite even under normal conditions [16]. The hydrated silica, i.e. silica hydrogel, formed by selective dissolution of the calcium provides favourable sites for apatite nucleation, as previously confirmed for glass-ceramic A-W [17–19]. Consequently, the glasses of compositions $3Fe_2O_3$,100CaO·SiO_2 (in weight ratio) with Na_2O, B_2O_3 and/or P_2O_5 added form an apatite layer on their surfaces with the rate increasing in the order CS + FeP < CS + FeNa < CS + FeB < CS + FeNaB < CS + FeNaP < CS + FeBP, in the simulated body fluid. The phosphate ion required for formation of the apatite layer is supplied from the surrounding fluid.

As described in Section 1, it has been shown that glasses and glass-ceramics forming an apatite layer on

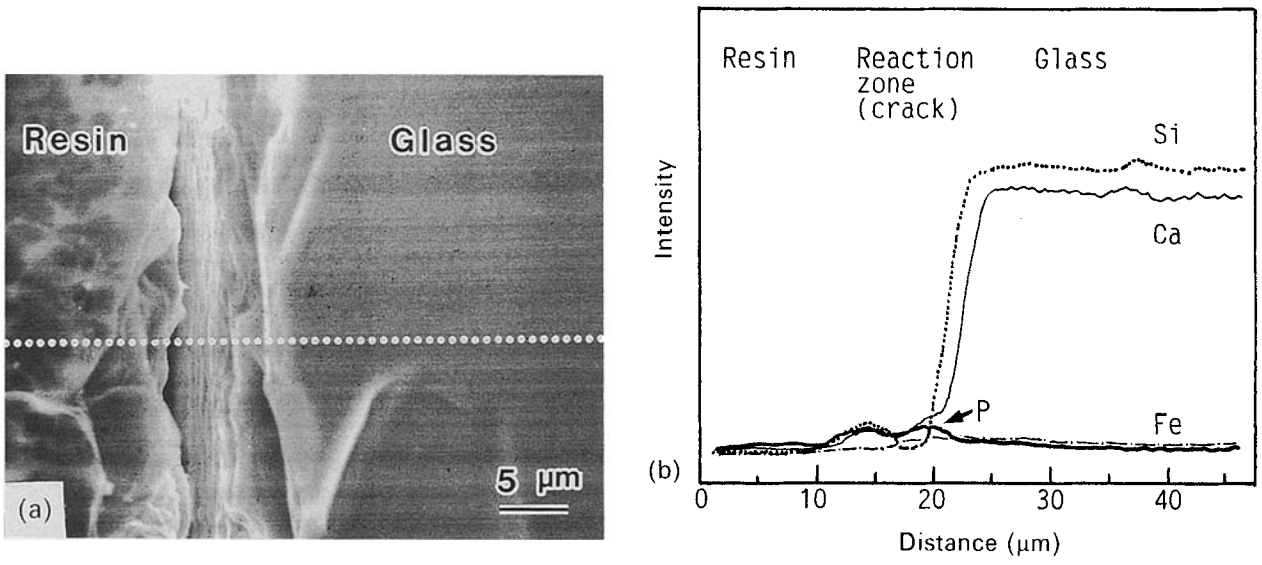

Figure 8 (a) SEM micrograph and (b) EPMA profile of a cross-section of glass CS + Fe soaked in simulated body fluid for 20 days.

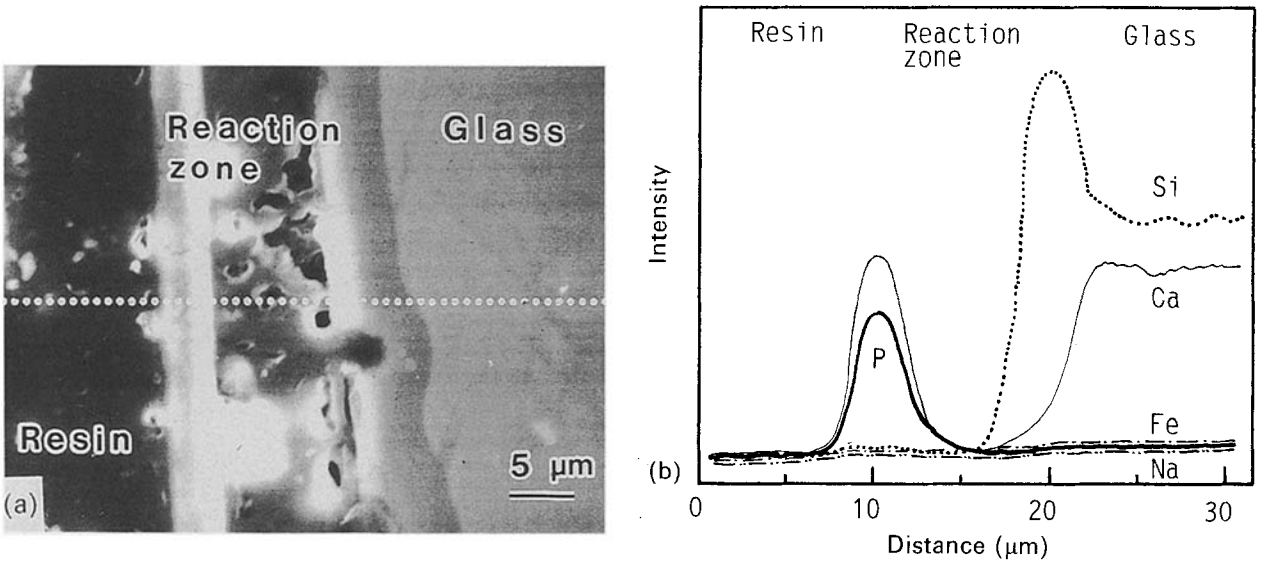

Figure 9 (a) SEM micrograph and (b) EPMA profile of a cross-section of glass CS + FeNa soaked in simulated body fluid for 20 days.

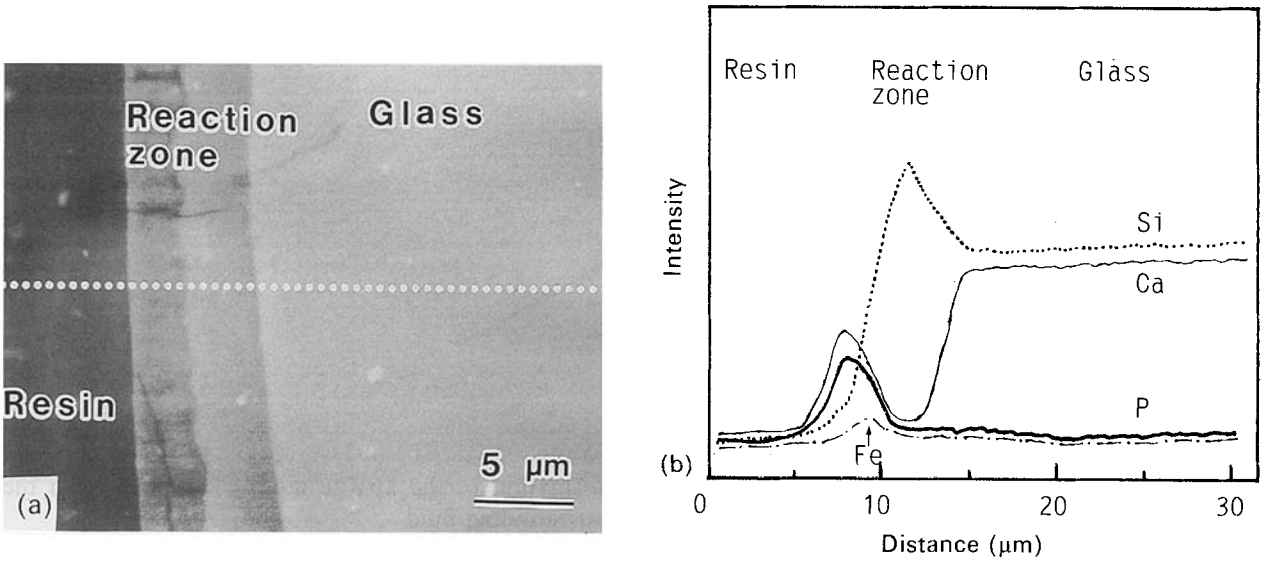

Figure 10 (a) SEM micrograph and (b) EPMA profile of a cross-section of glass CS + FeB soaked in simulated body fluid for 20 days.

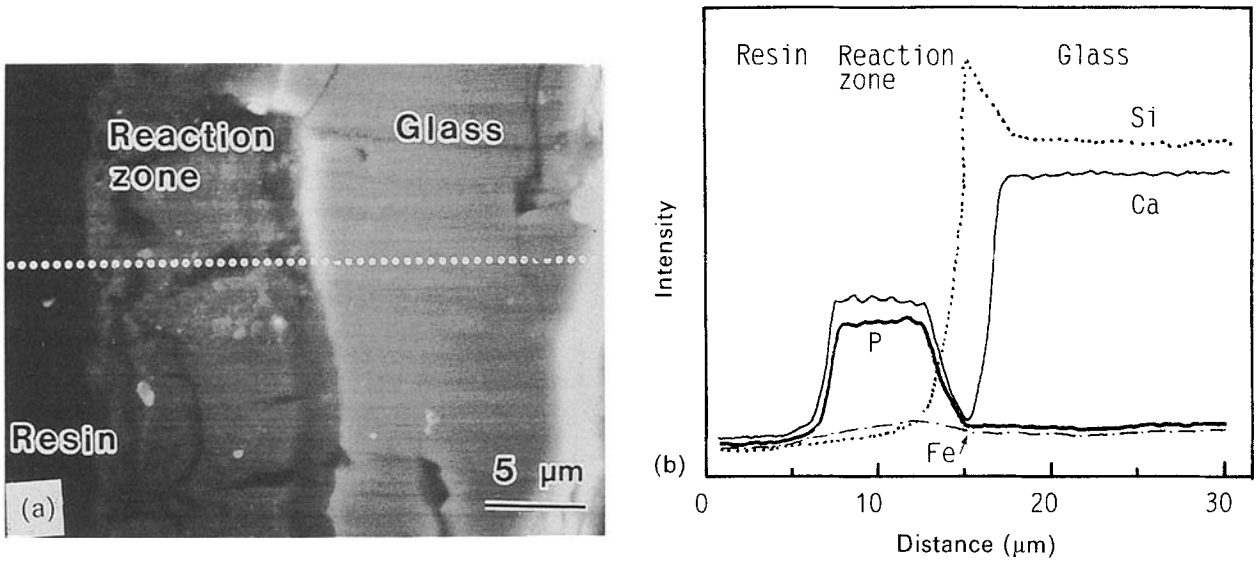

Figure 11 (a) SEM micrograph and (b) EPMA profile of a cross-section of glass CS + FeP soaked in simulated body fluid for 20 days.

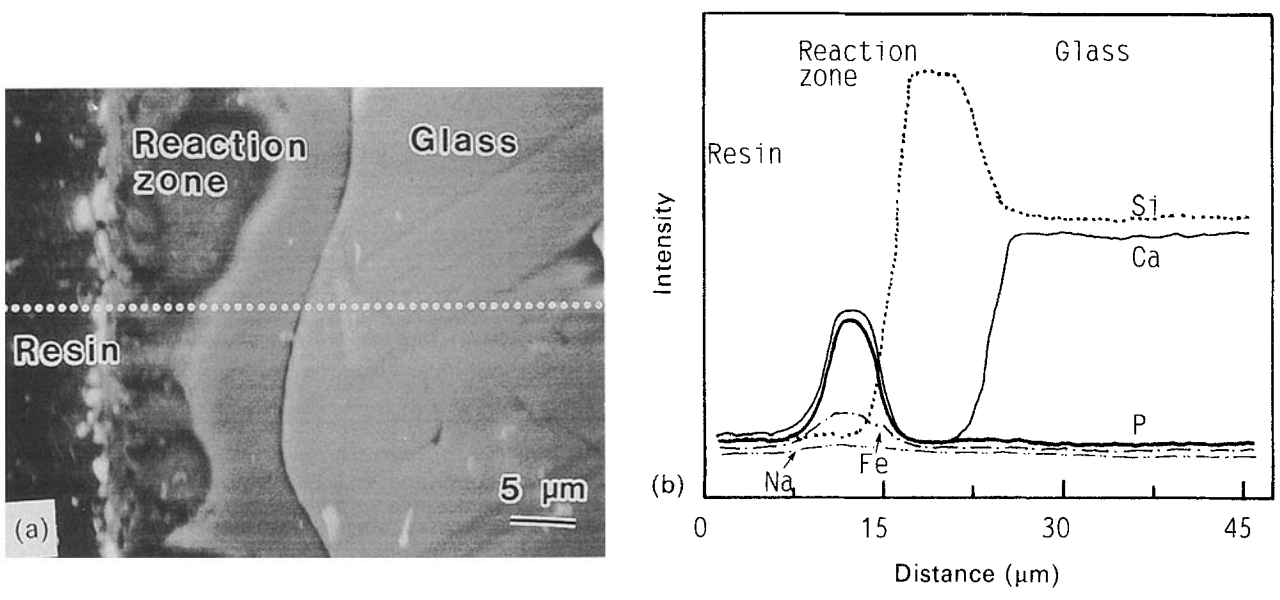

Figure 12 (a) SEM micrograph and (b) EPMA profile of a cross-section of glass CS + FeNaB soaked in simulated body fluid for 20 days.

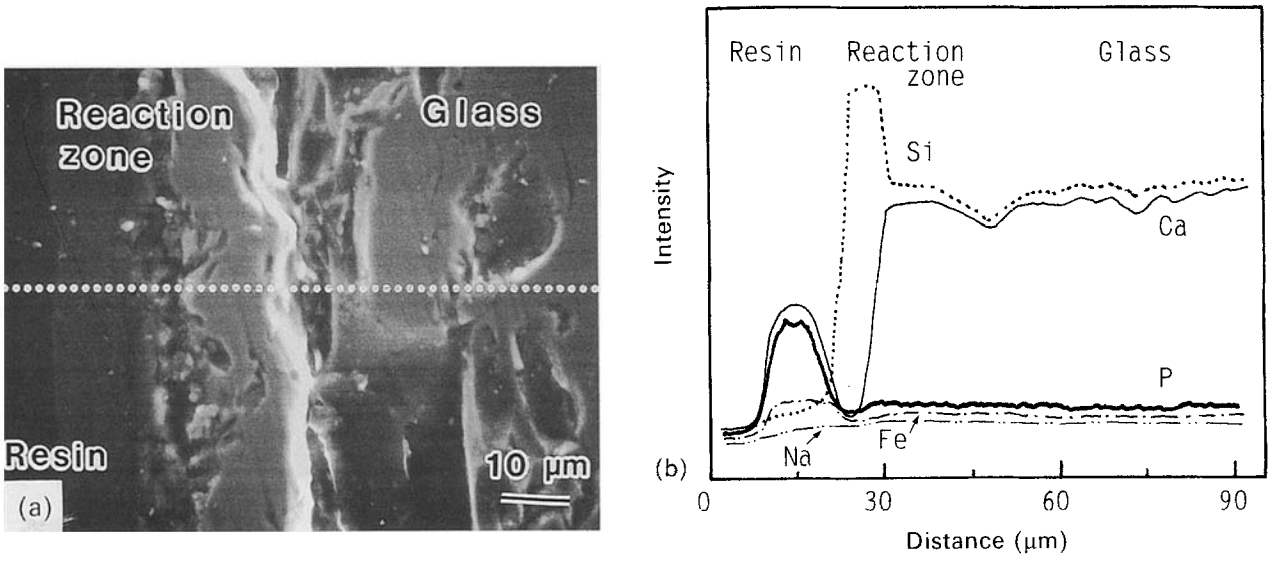

Figure 13 (a) SEM micrograph and (b) EPMA profile of a cross-section of glass CS + FeNaP soaked in simulated body fluid for 20 days.

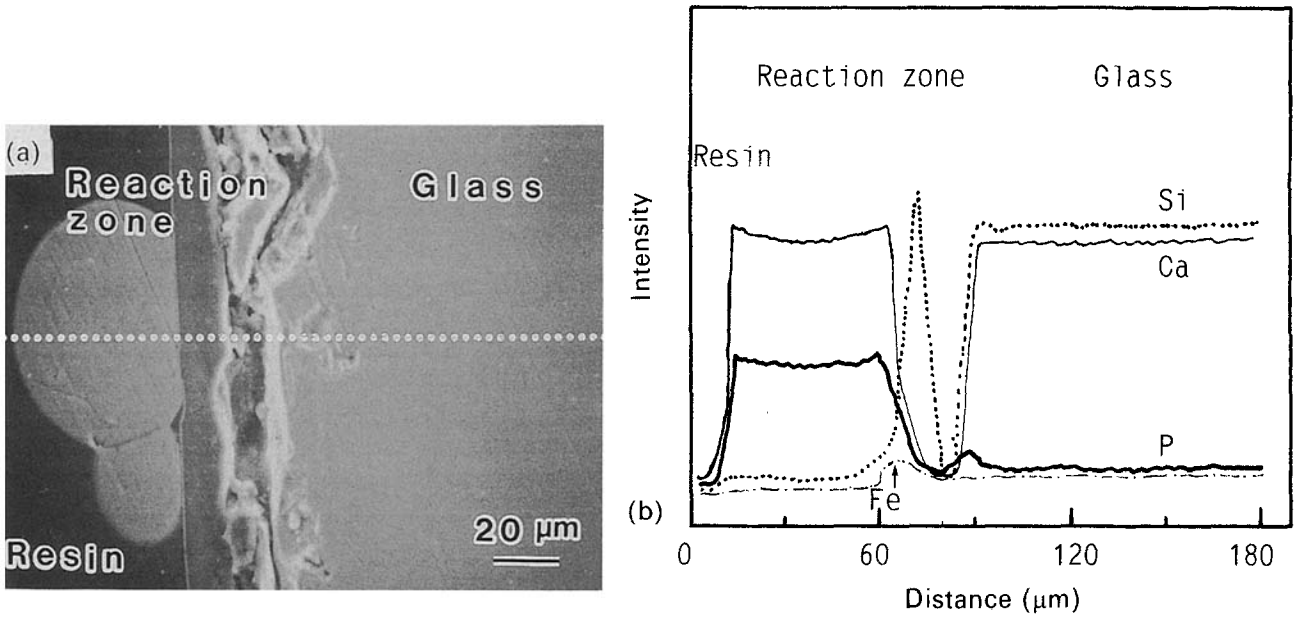

Figure 14 (a) SEM micrograph and (b) EPMA profile of a cross-section of glass CS + FeBP soaked in simulated body fluid for 20 days.

their surfaces in the simulated body fluid also bond to the bone, forming the same kind of the apatite layer in the living body [1–3, 5–13].

The present results, therefore, show that $3Fe_2O_3$,$100CaO \cdot SiO_2$ (in weight ratio) glasses with Na_2O, B_2O_3 and/or P_2O_5 added also bond to the bone, forming an apatite layer in the living body. This indicates that bioactive and ferrimagnetic glass-ceramics could be obtained from Fe_2O_3-containing $CaO–SiO_2$ glasses with Na_2O, B_2O_3 and/or P_2O_5 added.

Acknowledgement

This work was supported by a Grant-in-Aid for Scientific Research from The Ministry of Education, Science and Culture, Japan.

References

1. Y. EBISAWA, T. KOKUBO, K. OHURA and T. YAMAMURO, *J. Mater. Sci. Mater. Med.* **1** (1990) 239.
2. C. OHTSUKI, T. KOKUBO, K. TAKATSUKA and T. YAMAMURO, *Seramikkusu Ronbunshi* **1** (1991) 1.
3. K. OHURA, T. NAKAMURA, T. YAMAMURO, T. KOKUBO, Y. EBISAWA, Y. KOTOURA and M. OKA, *J. Biomed. Mater. Res.* **25** (1991) 357.
4. Y. EBISAWA, Y. SUGIMOTO, T. HAYASHI, T. KOKUBO, K. OHURA and T. YAMAMURO, *Seramikkusu Ronbunshi* **1** (1991) 7.
5. L. L. HENCH and A. E. CLARK, in "Biocompatibility of orthopedic implants", Vol. II, edited by D. F. Williams (CRC Press, Boca Raton, Florida, 1982) p. 129.
6. T. KOKUBO, T. HAYASHI, S. SAKKA, T. KITSUGI, T. YAMAMURO, M. TAKAGI and T. SHIBUYA, in "Ceramics in clinical applications", edited by P. Vincenzini (Elsevier, Amsterdam, 1987) p. 175.
7. T. KOKUBO, S. ITO, Z. T. HUANG, H. HAYASHI, S. SAKKA, T. KITSUGI and T. YAMAMURO, *J. Biomed. Mater. Res.* **24** (1990) 331.
8. T. KOKUBO, H. KUSHITANI, S. SAKKA, T. KITSUGI and T. YAMAMURO, *ibid.* **24** (1990) 721.
9. C. OHTSUKI, H. KUSHITANI, T. KOKUBO, S. KOTANI and T. YAMAMURO, *ibid.* **25** (1991) 1363.
10. T. KITSUGI, T. YAMAMURO, T. NAKAMURA, S. HIGASHI, Y. KOTANI, K. HIYAKUNA, S. ITO, T. KOKUBO, M. TAKAGI and T. SHIBUYA, *ibid.* **20** (1986) 1295.
11. T. KITSUGI, T. NAKAMURA, T. YAMAMURO, T. KOKUBO, T. SHIBUYA and M. TAKAGI, *ibid.* **21** (1987) 1255.
12. T. KITSUGI, T. YAMAMURO, T. NAKAMURA and T. KOKUBO, *ibid.* **23** (1989) 631.
13. T. KOKUBO, C. OHTSUKI, S. KOTANI, T. KITSUGI and T. YAMAMURO, in "Bioceramics", Vol. 2, edited by G. Heimke (German Ceramic Society, Cologne, 1990) p. 113.
14. J. GANBLE, in "Chemical anatomy, physiology and pathology of extracellular fluid", 6th Edn (Harvard University Press, Cambridge, Massachusetts, 1967) p. 1.
15. O. H. ANDERSSON, K. H. KARLSSON and K. KANGASNIEMI, *J. Non-Cryst. Solids* **119** (1990) 290.
16. W. NEUMAN and M. NEUMAN, in "The chemical dynamics of bone mineral" (University of Chicago, Chicago, 1958) p. 34.
17. T. KOKUBO, *J. Non-Cryst. Solids* **120** (1990) 138.
18. T. KOKUBO, H. KUSHITANI, C. OHTSUKI, S. SAKKA and T. YAMAMURO, *J. Mater. Sci. Mater. Med.* **3** (1992) 79.
19. *Idem, ibid.* **4** (1993) 1.

Received 4 November
and accepted 28 November 1991